

# Sensitivities of Low Energy Reactor Neutrino Experiments

Hau-Bin Li <sup>a,b</sup> and Henry T. Wong <sup>a,1</sup>

<sup>a</sup> Institute of Physics, Academia Sinica, Taipei 11529, Taiwan.

<sup>b</sup> Department of Physics, National Taiwan University, Taipei 10617,  
Taiwan.

## Abstract

The low energy part of the reactor neutrino spectra has not been measured experimentally. Its uncertainties limit the sensitivities in certain reactor neutrino experiments. This article discusses the origin of these uncertainties and examines their effects on the measurements of neutrino interactions with electrons and nuclei. The discrepancies between previous results and the Standard Model expectations can be explained by the under-estimation of the reactor neutrino spectra at low energies. To optimize the experimental sensitivities, measurements for  $\bar{\nu}_e$ -e cross-sections should focus on events with large ( $>1.5$  MeV) recoil energy while those for neutrino magnetic moment searches should emphasize on events  $<100$  keV. The merits and attainable accuracies for neutrino-electron scattering experiments using artificial neutrino sources are discussed.

**PACS Codes:** 14.60.Lm, 13.15.+g, 28.41.-i.

**Keywords:** Neutrino Properties, Neutrino Interactions, Fission Reactors.

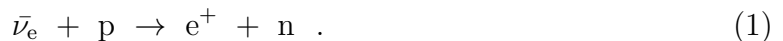
---

<sup>1</sup>Corresponding author: Email: htwong@phys.sinica.edu.tw; Tel:+886-2-2789-9682; FAX:+886-2-2788-9828.

# 1 Introduction

Nuclear power reactors are intense – and readily available – sources of electron anti-neutrinos ( $\bar{\nu}_e$ ) at the MeV energy range. They remain important tools in the experimental studies of neutrino properties and interactions.

Reactor-based neutrino oscillation experiments [1, 2] typically rely on the interactions between  $\bar{\nu}_e$  and proton, usually in the form of hydrogen in liquid scintillator:



With an interaction threshold of 1.8 MeV and a typical positron detection threshold of  $> 1$  MeV, the “reactor neutrino spectrum” [ $\phi(\bar{\nu}_e)$ ] above 3 MeV has to be known to derive the physics results.

There are by-now standard procedures for evaluating  $\phi(\bar{\nu}_e)$  using the reactor operation data. An accuracy of up to 1.4% between calculations and measurement has been achieved in the integrated flux [3]. The measured differential spectrum from the Bugey-3 experiment [4] was compared with three models of deriving  $\phi(\bar{\nu}_e)$ . The best one gave an accuracy of better than 5% from 2.8 MeV to 8.6 MeV neutrino energy, while the other two gave discrepancies at the 10-20% level in part of this energy range.

The conclusion of these studies is that  $\phi(\bar{\nu}_e)$  above 3 MeV can be considered to be calculable to the few % level. Therefore, long-baseline reactor neutrino oscillation experiments do not require “Near Detectors” for the flux normalization purpose. These experiments, including Chooz and Palo Verde which have been performed, KamLAND in operation and Borexino under construction, focus on the large mixing angles (big oscillation amplitudes) and small  $\Delta m^2$  parameter space.

However, the  $\phi(\bar{\nu}_e)$  below 3 MeV had neither been measured experimentally, nor thoroughly addressed theoretically. In Section 2, we summarize the essence of the calculations of reactor neutrino spectra, and describe the origins of the uncertainties at low energy. The potential contributions of these effects to the accuracies of experimental measurements are discussed. In particular, we investigate the case of neutrino-electron ( $\bar{\nu}_e$ -e) scatterings in Section 3, and show how the uncertainties in the low energy part of the reactor neutrino spectra limit the sensitivities in the cross-section measurements as well as the search of neutrino magnetic moments. The effects on the study of neutrino interactions on nuclei are discussed in Section 4. A list of relevant cross-sections scattered in the literature are compiled.

## 2 Reactor Neutrino Spectra

Electron anti-neutrinos are emitted in a nuclear reactor through  $\beta$ -decays of unstable nuclei produced by the fission of the four major fissile elements in the fuel:  $^{235}\text{U}$ ,  $^{238}\text{U}$ ,  $^{239}\text{Pu}$ ,  $^{241}\text{Pu}$ . Hundreds of different daughter nuclei are involved, each having its own decay life-time, branching ratio and Kurie distribution, some of which are not completely known. The inputs for calculating the overall  $\phi(\bar{\nu}_e)$  are derived from two alternative approaches: (I) modelings on the level densities and nuclear effects [5, 6], or (II) measurements of  $\beta$ -spectra due to neutron hitting the fissile isotopes [7]. The Bugey-3 experiment compared their data with these approaches [4] and concluded that the predictions of  $\phi(\bar{\nu}_e)$  from (II) are consistent with measurements at the  $<5\%$  level for  $E_{\nu} \sim 2.8\text{-}8.6$  MeV. The agreement between Approach (I) and data as well as among the two approaches are typically at the 10% level, and can deviate to the 20% level at part of the energy range. The Bugey-3 results contradicted those of Ref. [8] which claimed a discrepancy with (II) by 10% in spectral shape. In addition, recent studies on the non-equilibrium effects [9] suggested that the corrections may be as large as 25% for reactor neutrino oscillation experiments.

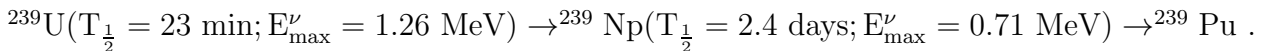
All these intensive and comprehensive efforts were motivated by oscillation studies with proton target [10, 11] via the interaction channel given in Eq. 1. They may be inadequate for the other experiments with reactor neutrinos. In particular, there are no measurements as well as systematic theoretical efforts on  $\phi(\bar{\nu}_e)$  below  $E_{\nu} \sim 2.8$  MeV. Existing compilations come from Refs. [6] and [12] which were derived from the summations of  $\beta$ -decays of fission fragments using different modelings. The calculated spectra below 3 MeV are displayed in Figure 1, showing that the models are consistent among themselves only to the 20% level. The discontinuities in the spectrum of Ref. [12] are due to the end-point effects of the many  $\beta$ -spectra.

There are many additional effects necessary to be considered in order to perform a correct evaluation of  $\phi(\bar{\nu}_e)$  at low energies. There are many more  $\beta$ -decays with  $Q$ -values less than 3 MeV that have to be modeled on with Approach (I). Similarly, the measurements with Approach (II) were performed with an exposure time for neutrons on  $^{235}\text{U}$  of 15 hours which is sufficient only to bring the  $\beta$ -activities above 3 MeV into equilibrium, and the measured  $\beta$ -spectra had a threshold of 2 MeV kinetic energy for the electrons. Consequently, fission products with live-times longer than 10 hours and  $\beta$ -decays with end-points less than 2 MeV are not accounted for. Examples of fission daughters belonging to this category include:  $^{97}\text{Zr}$  ( $E_{\text{max}}^{\nu} = 1.92$  MeV;  $\tau_{\frac{1}{2}} = 17$  h),  $^{132}\text{Te}$  ( $E_{\text{max}}^{\nu} = 2.14$  MeV;  $\tau_{\frac{1}{2}} = 78$  h) and  $^{93}\text{Y}$  ( $E_{\text{max}}^{\nu} = 2.89$  MeV;  $\tau_{\frac{1}{2}} = 10$  h).

The treatment is even more complicated for those with life-times comparable to a reactor cycle (12 to 18 months). During a typical reactor shut down, only a fraction

of the fuel elements are replaced, and the spent fuel is temporarily stored in the water tank within the reactor building (that is, in the vicinity of the experimental site). The old and new fuel elements are usually re-oriented within the core for the next cycle. The complications can be illustrated with a notable example. The fission daughter  $^{90}\text{Sr}$  has a half-life of 29.1 y and a cumulative yield of 5.4% per  $^{235}\text{U}$ -fission [13]. It would give rise to two subsequent  $\beta$ -decays with maximum  $E_\nu$  of 0.55 MeV and 2.27 MeV, respectively. Other examples include:  $^{106}\text{Ru}$  ( $E_{\text{max}}^\nu = 3.54$  MeV;  $\tau_{\frac{1}{2}} = 372$  d) and  $^{144}\text{Ce}$  ( $E_{\text{max}}^\nu = 3.00$  MeV;  $\tau_{\frac{1}{2}} = 285$  d).

Neutrons produced in fission can be absorbed by the fission fuel elements as well as by the surrounding materials. Some of the final states are unstable and can give rise to  $\beta$ -decays producing  $\bar{\nu}_e$ . There is also a smaller fraction of  $\nu_e$ 's due to isotopes which decay via electron captures and  $\beta^+$ -emissions [14]. Almost all such processes have Q-values below 3 MeV and hence contribute only to the low energy part of  $\phi(\bar{\nu}_e)$ . The major contribution from this category [11, 15] is expected to be from the reaction  $^{238}\text{U}(n, \gamma)^{239}\text{U}$ , leading to subsequent  $\beta$ -decays via



The typical  $\phi(\bar{\nu}_e)$  spectrum from the decays of  $^{239}\text{U}$  is displayed in Figure 1, showing that the flux is comparable to those due to  $\beta$ -decays of fission daughters. The complicated non-equilibrium effects for both Reactor ON and OFF periods [16] from the various neutron capture channels will contribute further to the uncertainties in the description of  $\phi(\bar{\nu}_e)$  at low energies. Meticulous book-keeping and complicated calculations are necessary to account for the various effects.

All these processes have not been quantitatively addressed. In addition, errors in the evaluation of  $\phi(\bar{\nu}_e)$  tend to be under-estimations due to some physical processes not accounted for. This would give rise to an excess of events which may mimic positive signatures for anomalous effects. Therefore, one should be cautious about the conceptual design of experiments and the interpretation of data where the low energy reactor  $\bar{\nu}_e$  plays a role, such as in neutrino-electron scatterings. Further work on the calculations of  $\phi(\bar{\nu}_e)$  at low energies and demonstrations of their accuracies would be of interest.

### 3 Neutrino-Electron Scatterings

Experiments on neutrino-electron ( $\bar{\nu}_e$ -e) scatterings

$$\bar{\nu}_e + e^- \rightarrow \bar{\nu}_e + e^- . \quad (2)$$

provide measurements of Standard Model parameters ( $g_V, g_A$ ) for electroweak interactions, as well as a probe to study the interference effects between the charged and neutral currents [17]. The process is also a sensitive way to study the electromagnetic form factors of neutrino interactions with the photons, and in particular, the neutrino magnetic moments [12]. The interaction vertex probed is the same as that giving rise to neutrino radiative decays [18]:  $\nu_1 \rightarrow \nu_2 + \gamma$ , providing sensitivities competitive even to the limits derived in supernova SN1987a [19].

The experimental observable is the kinetic energy of the recoil electrons( $T$ ). Following Ref. [12], the differential cross section is given by :

$$\frac{d\sigma}{dT}(\nu - e) = \left(\frac{d\sigma}{dT}\right)_{SM} + \left(\frac{d\sigma}{dT}\right)_{MM} . \quad (3)$$

The Standard Model(SM) term is

$$\left(\frac{d\sigma}{dT}\right)_{SM} = \frac{G_F^2 m_e}{2\pi} [(g_V + g_A)^2 + (g_V - g_A)^2 \left[1 - \frac{T}{E_\nu}\right]^2 + (g_A^2 - g_V^2) \frac{m_e T}{E_\nu^2}] \quad (4)$$

where  $g_V = 2 \sin^2 \theta_W - \frac{1}{2}$  and  $g_A = -\frac{1}{2}$  for  $\nu_\mu$ -e and  $\nu_\tau$ -e scatterings which proceed via neutral-current interactions only, while  $g_V \rightarrow g_V + 1$  and  $g_A \rightarrow g_A + 1$  for  $\nu_e$ -e scatterings, where both charged and neutral currents are involved. The expression can be modified for  $\bar{\nu}$ -e scatterings by the replacement  $g_A \rightarrow -g_A$  to account for the effects due to different helicities. The magnetic moment(MM) term is a non-Standard Model process given by

$$\left(\frac{d\sigma}{dT}\right)_{MM} = \frac{\pi \alpha_{em}^2 \mu_\nu^2}{m_e^2} \left[ \frac{1 - T/E_\nu}{T} \right] \quad (5)$$

where the neutrino magnetic moment  $\mu_\nu$  is often expressed in units of the Bohr magneton( $\mu_B$ ). The process can be due to *diagonal* and *transition* magnetic moments, which change only the spins and both the spins and flavors, respectively. The MM term has a  $1/T$  dependence and hence dominates at low electron recoil energy. The expected recoil differential spectra for both processes are depicted in Figure 2a. At energy transfer comparable to the inner-shell binding energies of the target, a small and known correction factor has to be applied to the cross-section formulae [20]. The spectra below 2 keV are due to the neutrino coherent scatterings on nuclei [1, 21], derived from Eqs. 14 and 15 to be discussed further in Section 4.

Experimentally, the interactions of  $\nu_\mu$ -e/ $\bar{\nu}_\mu$ -e [22] and  $\nu_e$ -e [23] have been studied with high energy and intermediate energy accelerator neutrinos. Although  $\bar{\nu}_e$ -e have been observed with reactor neutrinos [24, 25, 26], the MeV-energy range is still a relatively untested range where there are still big uncertainties in the measured cross-sections. Indeed, the results of Ref. [24] give rise to different levels of consistencies (or slight discrepancies) with the Standard Model expectations when different  $\phi(\bar{\nu}_e)$  were used [6, 12, 24, 27]. There are various current experiments [28, 29, 30] pursuing this subject.

### 3.1 Reactor Neutrinos: $\bar{\nu}_e$ -e Scatterings

In this Section, we investigate the effects of uncertainties in  $\phi(\bar{\nu}_e)$  to the sensitivities of SM cross-section measurements and limits of MM searches. The prescriptions for evaluating  $\phi(\bar{\nu}_e)$  from Ref. [12] were adopted. Since only the relative errors are considered, the conclusions would be independent of the fine details of the models used. The uncertainties in  $\phi(\bar{\nu}_e)$  were parametrized by two variables  $\xi$  and  $\Delta$  such that the spectra above and below  $\xi$  are taken to be accurate to 5% and  $\Delta\%$ , respectively.

The correlations between electron recoil energy (T) and neutrino energy ( $E_\nu$ ) for both SM and MM processes (Eqs. 4 and 5, respectively) due to  $\phi(\bar{\nu}_e)$  are displayed in Figure 3a and 3b, respectively. Both distributions peak at small  $E_\nu$  and T. The contours represent equipartition levels of event rates normalized to the largest value at the innermost contour. It can be seen that (1) most  $\bar{\nu}_e$ -e events for both SM and MM are of low recoil energies, and (2) they are mostly due to interactions by low energy neutrinos, the contributions of which are more pronounced in MM than in SM. As illustrations, 84%, 64% and 29% of the  $\bar{\nu}_e$ -e SM scattering events at 100 keV recoil energy are due to neutrinos with energy less than 3, 2 and 1 MeV, respectively.

The overall accuracy ( $\delta_{\text{total}}$ ) in a typical reactor experiment depends on: (a) the contributions from the uncertainties of  $\phi(\bar{\nu}_e)$  to the SM ( $\delta_{\text{SM}}$ ) and MM ( $\delta_{\text{MM}}$ ) cross-sections, and (b) the measurement uncertainties ( $\delta_{\text{det}}$ ) which include the combined effects of the experimental systematic and statistical errors, including those introduced in Reactor ON–OFF subtraction. In the case where the MM contributions are negligible, one can write

$$\delta_{\text{total}}^2 = \delta_{\text{det}}^2 + \delta_{\text{SM}}^2 . \quad (6)$$

To achieve reasonable statistical accuracy, most experiments compare data above a certain detection threshold with the integrated cross-sections. The integral recoil spectra for different threshold is shown in Figure 2b. The SM contribution is of the order of  $1 \text{ kg}^{-1}\text{day}^{-1}$  at the typical parameters for reactor experiments and detection threshold of 100 keV

With the conservative but realistic values of  $\Delta=30\%$  and  $\xi=3 \text{ MeV}$ , the attainable total “1- $\sigma$ ” accuracies for the SM cross-sections are evaluated and depicted in Figure 4a as a function of detection threshold for different values of the measurement error  $\delta_{\text{det}}$ . Also shown are sensitivities for the detection ranges of  $R_1=5\text{-}100 \text{ keV}$  and  $R_2=0.5\text{-}2 \text{ MeV}$ , which correspond to the ranges of the on-going experiments Kuo-Sheng [29] and MUNU [28], respectively. It can be seen that, for the same  $\delta_{\text{det}}$ , measurements with a low threshold are limited by the uncertainties in  $\phi(\bar{\nu}_e)$ . An experiment optimized for SM cross-section measurements should focus on the events with higher recoil energy (above 1.5 MeV) while

trying to compensate for the loss of statistical accuracy with large target mass, that is, keeping the threshold high without compromising  $\delta_{\text{det}}$ .

In an analysis for the magnetic moment effects, the contributions from  $\delta_{\text{MM}}$  should be taken into consideration. Since the uncertainties in the evaluation of  $\phi(\bar{\nu}_e)$  will translate into correlated errors of the same sign for both  $\delta_{\text{SM}}$  and  $\delta_{\text{MM}}$ , the combined experimental uncertainties can be written as

$$\delta_{\text{total}}^2 = \delta_{\text{det}}^2 + (\delta_{\text{SM}} + \delta_{\text{MM}})^2 . \quad (7)$$

In other words, an under-estimation of  $\phi(\bar{\nu}_e)$  would lead to an excess of events after Reactor ON/OFF subtraction, which can be taken as signatures of positive magnetic moments. The positive signals would be interpreted as even bigger values of  $\mu_\nu$  when the *same* under-estimated  $\phi(\bar{\nu}_e)$  is used to evaluate the magnetic moment.

The attainable MM limits at 90% confidence level (CL) can be derived from  $\delta_{\text{total}}$ , and are displayed in Figure 4b as a function of threshold and for different values of  $\delta_{\text{det}}$ . The sensitivities trend is distinctively different from that of SM cross-section measurements in Figure 4a. The SM cross-section becomes “background” to MM searches, such that in the energy range where SM interactions dominate, the SM uncertainties will get amplified by the big SM:MM ratio in the derivation of magnetic moments. The MM effects, therefore, should be investigated at regions where MM is much larger than SM, that is, at low recoil energies. The structures at 1-3 MeV for small  $\delta_{\text{det}}$  are due to the sharp transition at  $\xi=3$  MeV in modeling the  $\phi(\bar{\nu}_e)$  uncertainties. A more realistic description is that  $\Delta$  would increase continuously as  $E_\nu$  drops below 3 MeV.

Figure 4b indicates several strategic features in the experimental search for neutrino magnetic moments with reactor neutrinos. In the scenario where  $\delta_{\text{det}}=30\%$ , (1) experiments with threshold of  $>1$  MeV recoil energy cannot probe below  $10^{-10} \mu_B$ , (2) experiments with range  $R_2$  cannot probe below  $1.2 \times 10^{-10} \mu_B$ , and (3) a sensitive search should be conducted with as low a threshold as possible and preferably with a high energy cut-off. The sensitive region can approach  $3 \times 10^{-11} \mu_B$  for the  $R_1$  range.

To investigate the effects of  $\Delta$  keeping  $\xi=3$  MeV, the sensitivities for both SM cross section measurements and MM limits are shown in Figures 5a and 5b, respectively. The special case of  $\delta_{\text{det}}=0\%$  is chosen to characterize a *perfect* experiment where the sensitivities are limited only by the uncertainties of  $\phi(\bar{\nu}_e)$ . The differences in the attainable sensitivities among the different energy ranges are very distinct between the two measurements. A high threshold value provides best sensitivities in SM cross-sections while a restricted low energy range  $R_1$  is optimal for MM searches. As depicted in Figure 5a, a  $\delta_{\text{total}} < 10\%$  SM measurement is in principle possible with a high threshold ( $>1.5$  MeV) experiment even for  $\Delta=30\%$ . In this case, the sensitivities are limited by experimental

uncertainties  $\delta_{\text{det}}$  instead. On the other hand, measurements with low energy data will require improving  $\Delta$  to better than 10% to achieve the same sensitivities.

Figure 5b shows that the R<sub>1</sub>-class of experiments are the least sensitive to the uncertainties in  $\phi(\bar{\nu}_e)$ , even for very big  $\Delta$ . If the entire range of  $\phi(\bar{\nu}_e)$  can be known to 5%, such experiments can probe the region down to  $10^{-11} \mu_B$ . In contrast, the goals of the R<sub>2</sub>-class experiments for achieving better than  $10^{-10} \mu_B$  should be complemented by a demonstration of the control of the low energy part of the reactor neutrino spectrum to the <20% level.

The effects of the uncertainties in  $\phi(\bar{\nu}_e)$  on the derived magnetic moment limits were not discussed in previous work [24, 25, 26]. The  $\bar{\nu}_e$ -e reactor experiment in Ref [24] had a threshold of 1.5 MeV and an uncertainty in the SM cross-section measurement of  $\delta_{\text{det}}=29\%$ . A reanalysis of this experiment in Ref [12] with improved input parameters on  $\phi(\bar{\nu}_e)$  and  $\sin^2\theta_W$  gave a positive signature consistent with the interpretation of a finite magnetic moment at  $(2 - 4) \times 10^{-10} \mu_B$ . A possibility to mimic the effect of a neutrino magnetic moment at  $2 \times 10^{-10} \mu_B$  could be an under-estimation of  $\phi(\bar{\nu}_e)$  by  $\Delta=57\%$  below 3 MeV. Taking this value of  $\Delta$  to be the characteristic uncertainties of  $\phi(\bar{\nu}_e)$  at low energies, one can infer from Figure 5b that the attainable sensitivities for  $\mu_\nu$  for R<sub>1</sub>- and R<sub>2</sub>-classes of experiments are  $4 \times 10^{-11} \mu_B$  and  $1.6 \times 10^{-10} \mu_B$ , respectively. Similarly, measurements from Ref. [26] were performed in the range of 500 keV to 2 MeV, and had an experimental uncertainty of  $\delta_{\text{det}}=50\%$ . The quoted upper limit of  $1.5 \times 10^{-10} \mu_B$  at 68% CL corresponds to a maximum allowed  $\Delta=65\%$ . With future experiments probing the level of  $\mu_\nu < 10^{-10} \mu_B$ , it will be necessary to take into account the uncertainties in  $\phi(\bar{\nu}_e)$ .

It should be emphasized that the “attainable sensitivities” presented in this section are derived from measurements of integrated cross-sections within a specified energy range of electron recoil energy (that is, counting experiments). In the cases where statistics are abundant enough for differential cross-section measurements to become possible, sensitivities can be further enhanced by considering the spectral shape. Nevertheless, the generic conclusions are still valid: (a) experiments for SM cross-section measurements should focus on large (>1.5 MeV) recoil energies, where the events are due mostly to the  $E_\nu > 3$  MeV which is well-modeled, and (b) experiments for MM searches should focus on the R<sub>1</sub>-class energy ranges, where the uncertainties from SM contributions are minimized, and the  $\frac{1}{T}$  spectral shape would provide further constraints.

Technically, the R<sub>1</sub>-class experiments would be similar to those for the searches of Cold Dark Matter [2]. The new challenges are to control the ambient background in a surface site – *and* in the vicinity of a power reactor core. Detectors with high-purity germa-

mium crystals [29, 30] and crystal scintillators [29] have been discussed. An experimental program is being pursued at the Kuo-Sheng Reactor in Taiwan [29].

### 3.2 Neutrino Source: $\nu_e$ -e Scatterings

Experiments on  $\nu_e$ -e scatterings have been performed at medium energy accelerators [23]. Sources of  $\nu_e$  from  $^{51}\text{Cr}$  have been produced for calibrating the gallium solar neutrino experiments [31].

Studies of neutrino magnetic moments with artificial neutrino sources have been discussed [32, 33]. In a similar spirit, the sensitivities on SM cross section measurements and MM limits using a  $\nu_e$  mono-chromatic source are studied. The differential cross-sections for both SM and MM at  $10^{-10} \mu_B$  are shown in Figure 6 for two illustrative cases:  $^{51}\text{Cr}$  at 750 keV and  $^{55}\text{Fe}$  at 230 keV. The attainable MM limits as a function of  $E_\nu$  for different  $\delta_{\text{det}}$  are shown in Figure 7. The detection threshold for the recoil electrons is taken to be 1 keV. The values of  $\delta_{\text{det}}$  represent the combined uncertainties due to the experiments and the measurements of source strength. For instance, if a 1% measurement can be made, the MM sensitivities of  $< 10^{-11} \mu_B$  may be probed.

In principle, experiments with neutrino sources allows better systematic control and more accurate “SOURCE-OFF” background measurements. Specific spectral shape for the final-state measurables can be studied. For instance, the energy of the final-state electron spectra in  $\nu_e$ -N charged-current interactions would also be delta-functions, as considered in the calibration measurements in the proposed LENS project [34]. An interesting extension to the  $\nu_e$ -e scattering studies is the study of the “Compton” edges due to scatterings of the mono-energy  $\nu_e$ , an experimentally cleaner signature.

To probe MM sensitivities to the  $10^{-12} \mu_B$  level and beyond, new technologies such as the various cryogenic detectors with much lower (100 eV or less) detection threshold have to be developed – a formidable experimental challenge. The “neutrino-related-background” at very low energies will be dominated by the coherent scatterings on nuclei in reactor neutrino experiments. The spectra below 2 keV shown in Figure 2a are due to coherent scatterings of reactor  $\bar{\nu}_e$  on germanium, assuming a complete detection of the total recoil energy (typical ionization yield for germanium at this energy range is only about 0.2–0.3). To minimize the contributions of the SM background of *both*  $\nu$ -e and  $\nu$ -N coherent scatterings, low energy neutrino sources will be appropriate. Schemes are considered using tritium  $\bar{\nu}_e$  source where  $E_{\text{max}}^\nu = 18.6$  keV [33]. Reactor neutrinos can still be of use only if the detectors can provide very good event identification capabilities, such as the pulse shape discrimination (PSD) techniques, to differentiate electrons from

nuclear recoils.

However, the statistical accuracy should also be put into consideration in realistic experiments. A neutrino “point” source of 1 MCi strength placed at the center of a spherical detector of radius 1 m is equivalent to an exposure to a homogeneous flux of  $8.8 \times 10^{11} \text{ cm}^{-2}\text{s}^{-1}$ , as compared to that for typical reactor experiments at  $10^{13} \text{ cm}^{-2}\text{s}^{-1}$ . Coupled with the tremendous efforts and expenses of producing the neutrino sources as well as their finite life-times (for instance,  $\tau_{\frac{1}{2}} = 28$  days for  $^{51}\text{Cr}$ ), reactor neutrinos still offer advantages in the study of low energy neutrino physics.

For completeness and comparison, we mention that nuclear power reactors also produce  $\nu_e$  [14], expected to be predominantly from  $^{51}\text{Cr}$  and  $^{55}\text{Fe}$  via neutron activation of the equipment and building materials, at the estimated level of about  $10^{-3} \nu_e/\bar{\nu}_e$ . The effects from the small contaminations of  $\nu_e$  on the measurements of  $\bar{\nu}_e$  are therefore negligible. Since the unstable parent isotopes have relatively long half-lives, experimental studies with  $\nu_e$  can in principle be performed by studying the transient effects *after* the reactor is switched OFF, where the signatures would have the characteristic half-lives, such as that of 28 days in the case of  $\nu_e$ 's from  $^{51}\text{Cr}$ . Such experiment has been considered for studying the possible anomalous matter effects of  $\nu_e$  which may be absent in  $\bar{\nu}_e$  [35].

## 4 Neutrino Interactions on Nuclei

Neutrino cross-sections on nuclei is another subject which can be studied with reactor neutrinos. The charged- and neutral-current interactions on deuteron have been experimentally measured [36], while neutral-current excitations have been studied theoretically [37]. The  $\bar{\nu}_e\text{N}$  charged-current interactions have also been discussed in connection to the detection of low energy  $\bar{\nu}_e$  from the Earth [38]. It is therefore relevant to study the attainable accuracies of these cross-sections with reactor neutrinos under the scenarios mentioned above.

The neutral-current excitation processes:

$$\bar{\nu}_e + \text{N} \rightarrow \bar{\nu}_e + \text{N}^* \quad (8)$$

have the dependence of

$$\sigma(E_\nu) \propto (E_\nu - E_{\text{ex}})^2 \quad (9)$$

where  $E_{\text{ex}}$  is the threshold excitation energy. It has been observed only in the case of  $^{12}\text{C}$  with accelerator neutrinos [39]. Theoretical work [40] suggests that these cross sections

are sensitive to the axial isoscalar component of the weak neutral-current interactions and the strange quark content of the nucleon.

The attainable accuracies as a function of  $E_{\text{ex}}$  at  $\delta_{\text{det}} = 0$  for different values of  $\Delta$  are displayed in Figure 8. To achieve a 10% accuracy in the cross-section measurement in the most promising case for the M1 transition in  ${}^7\text{Li}$  ( $E_{\text{ex}} = 448$  keV), it is necessary to evaluate the low energy part of  $\phi(\bar{\nu}_e)$  to better than 16%.

Neutrino disintegrations on deuteron involve three-body final states:

$$\bar{\nu}_e + {}^2\text{H} \rightarrow \text{n} + \text{n} + \text{e}^+ \quad (E_{\text{T}} = 4.03 \text{ MeV}) , \quad (10)$$

and

$$\bar{\nu}_e + {}^2\text{H} \rightarrow \bar{\nu}_e + \text{p} + \text{n} \quad (E_{\text{T}} = 2.226 \text{ MeV}) \quad (11)$$

for the charged- ( $\bar{\nu}_e\text{dCC}$ ) and neutral-current ( $\bar{\nu}_e\text{dNC}$ ) channels, respectively. The dependence on the threshold energy  $E_{\text{T}}$  is modified to

$$\sigma(E_\nu) \propto \int \sqrt{E_{\text{r}}} (E_\nu - E_{\text{T}} - E_{\text{r}} + m) [(E_\nu - E_{\text{T}} - E_{\text{r}} + m)^2 - m^2]^{\frac{1}{2}} dE_{\text{r}} , \quad (12)$$

where  $E_{\text{r}}$  is the reduced kinetic energy of the final proton and neutron, and  $m=m_e$  and 0 for  $\bar{\nu}_e\text{dCC}$  and  $\bar{\nu}_e\text{dNC}$ , respectively. There is a sharp increase in the cross-section for  $\bar{\nu}_e\text{dNC}$  near threshold, such that only 0.43% of the events in a reactor experiment would originate from  $\bar{\nu}_e$  of  $E_\nu < 3$  MeV. Accordingly, the attainable accuracies in both channels are limited only by the uncertainties of the high energy part of  $\phi(\bar{\nu}_e)$ , which is about 5%. These uncertainties are better than the experimental errors [36] achieved at present.

One can extend the studies to the generic case where the neutrino interactions do not have thresholds but possess an energy dependence parametrized by an index  $n$ , such that

$$\sigma_{\nu\text{N}}(E_\nu) \propto E_\nu^n . \quad (13)$$

The attainable accuracies for an integral cross-section measurement for different values of  $n$  as a function of  $\Delta$  are displayed in Figure 9. As expected, cross-sections with large  $n$  favor large  $E_\nu$  such that the accuracies approach that of  $\phi(\bar{\nu}_e)$  at high energy. Interactions with  $n \leq -1$ , on the other hand, are dominated by small  $E_\nu$  and the uncertainties are given by  $\Delta$ .

As indicated in Figure 2a, the coherent scatterings of low energy neutrinos on nuclei limit the  $\bar{\nu}_e\text{-e}$  threshold and therefore the MM sensitivities in reactor neutrino experiments. The corresponding cross sections due to the SM and MM processes are [21]:

$$\left(\frac{d\sigma}{dT}\right)_{\text{SM}}^{\text{coh}} = \frac{G_{\text{F}}^2}{4\pi} m_{\text{N}} [Z(1 - 4\sin^2\theta_{\text{W}}) - N]^2 \left[1 - \frac{m_{\text{N}} T_{\text{N}}}{2E_\nu^2}\right] \quad \text{and} \quad (14)$$

$$\left(\frac{d\sigma}{dT}\right)_{\text{MM}}^{\text{coh}} \sim \frac{\pi\alpha_{\text{em}}^2\mu\nu^2}{m_e^2}Z^2\left[\frac{1-T/E_\nu}{T}\right], \quad \text{respectively,} \quad (15)$$

where  $m_N$ ,  $N$  and  $Z$  are the mass, neutron number and atomic number of the nuclei, respectively, and  $T_N$  is their recoil energy. Both of the  $\sim N^2$  and  $Z^2$  dependences signify coherence. This SM interaction is of significance in astrophysical processes but has not yet been observed in an experiment due to the extremely small energy depositions in nuclear recoils. It dominates over the  $\bar{\nu}_e$ -e scatterings at recoil energy less than  $\sim 1$  keV. The integral SM cross-section is characterized by  $n=2$  such that at  $\Delta=30\%$ , a cross-section measurement with an accuracy of 15% can be achieved in a reactor-based experiment. The effects of magnetic moments at  $10^{-10} \mu_B$  in the coherent scattering channel are relevant only at recoil energy less than 10 eV.

## 5 Summary and Discussion

The strong and positive evidence of neutrino oscillations implies the existence of neutrino masses and mixings, the physical origin, structures and experimental consequences of which are still not thoroughly known or understood.

Experimental studies on the neutrino properties and interactions which may reveal some of these fundamental questions are therefore of interest and relevance. Nuclear power reactors remain the most available and intense sources of neutrinos, and can contribute to these studies. The low energy (MeV scale) and that being related to the first family (and therefore allowing the possibility of anomalous matter effects) may favor exotic phenomena to manifest themselves. The low energy part of the reactor neutrino spectra has not been well modeled. To study detection channels other than  $\bar{\nu}_e$  on proton, the  $\phi(\bar{\nu}_e)$  at low energy will have to be worked out and the accuracies shown to be in control. Future work along this direction will be of interest.

In this article, we discussed the origins of the uncertainties in the modeling of the low energy reactor neutrino spectra. Neutrino emissions from long-lived isotopes as well as from final states due to neutron excitations have to be taken into account. We studied how the uncertainties may limit the sensitivities in measurements of reactor neutrino with electrons and nuclei. The discrepancies between the results of Ref. [24] and the analysis of Ref. [12] can be explained by the under-estimation of the low energy part of  $\phi(\bar{\nu}_e)$  by 57%.

To optimize the cross-section measurements for  $\bar{\nu}_e$ -e scatterings, one should focus on the high energy ( $>1.5$  MeV) electron recoil events. For magnetic moment searches, it would be best to restrict to the  $<100$  keV range where the effects due to the uncertainties of

the Standard Model “background” are mostly decoupled. On the other hand, experiments which rely on the intermediate energy range of 0.5 to 2 MeV will be limited in sensitivities in both cross-section measurements and magnetic moment searches – unless the precision of the low energy reactor neutrino spectra is demonstrated. An experimental program adopting these strategies is being pursued at the Kuo-Sheng Power Reactor Plant [29]. A high-purity germanium detector is employed to optimize the detector threshold while CsI(Tl) crystal scintillators are adopted to study the high energy events taking advantage of their many potential merits [41] such as large available mass and yet being compact in size.

Artificial neutrino sources are attractive alternatives which may offer better systematic control. The event rates tend to be less than those with reactor neutrinos, unless both the source and the detector can be made very compact. For similar uncertainty levels on the source strength, the attainable sensitivities in both cases are comparable. To achieve the  $10^{-12} \mu_B$  range and beyond for magnetic moment searches, very low energy neutrino sources such that tritium is more appropriate, complemented with new detector technology with the range of 10-100 eV threshold.

## 6 Acknowledgements

The authors would like to thank P. Vogel for stimulating discussions and information on the evaluations of reactor neutrino spectra. We are grateful to S. Pakvasa, F. Vannucci, Z.Y. Zhou and J. Li for their valuable input. This work was supported by contracts NSC 89-2112-M-001-056 and NSC 90-2112-M-001-037 from the National Science Council, Taiwan. The support of H.B. Li is from contracts NSC 90-2112-M002-028 and MOE 89-N-FA01-1-0 under P.W.Y. Hwang.

## References

- [1] For a textbook survey, see, for example, “Physics of Massive Neutrinos”, 2nd Edition, F. Boehm and P. Vogel, Cambridge University Press (1992), and references therein.
- [2] For the recent status, see, for example, *Proc. of XIXth Conf. on Neutrino Phys. & Astrophys.*, eds. J. Law, R.W. Ollerhead and J.J. Simpson, Nucl. Phys. **B** (Procs. Suppl.) **91** (2001), and references therein.
- [3] Y. Declais et al., Phys. Lett. **B 338**, 383 (1994).
- [4] B. Achkar et al., Phys. Lett. **B 374**, 243 (1996).
- [5] B.R. Davis et al., Phys. Rev. **C 19**, 2259 (1979);  
P. Vogel et al., Phys. Rev. **C 24**, 1543 (1981);  
H.V. Klapdor and J. Metzinger, Phys. Rev. Lett. **48**, 127 (1982);  
H.V. Klapdor and J. Metzinger, Phys. Lett. **B 112**, 22 (1982);  
O. Tengblad et al., Nucl. Phys. **A 503**, 136 (1989).
- [6] F.T. Avignone and Z.D. Greenwood, Phys. Rev. **C 22**, 594 (1980).
- [7] K. Schreckenbach et al., Phys. Lett. **B 160**, 325 (1985);  
A.A. Hahn et al., Phys. Lett. **B 218**, 365 (1989).
- [8] Yu.V. Klimov et al., Sov. J. Nucl. Phys. **52(6)**, 994 (1990).
- [9] V.I. Kopeikin, L.A. Mikaelyan, and V.V. Sinev, Phys. Atomic Nuclei **64**, 849 (2001).
- [10] P. Vogel, Phys. Rev. **D 29**, 1918 (1984).
- [11] V.I. Kopeikin, L.A. Mikaelyan, and V.V. Sinev, Phys. Atomic Nuclei **60**, 172 (1997).
- [12] P.Vogel and J.Engel, Phys. Rev. **D 39**, 3378 (1989).
- [13] T.R. England and B.F. Rider, Evaluation and Compilation of Fission Yields, LA-UR-94-3106 (1994).
- [14] S.M. Blankenship, Internal Report, UC Irvine (1976);  
K. Schreckenbach, Internal Report, ILL Grenoble (1984).
- [15] A.M. Bakalyarov, V.I. Kopeikin, and L.A. Mikaelyan, Phys. Atomic Nuclei **59**, 1171 (1996).
- [16] V.I. Kopeikin, L.A. Mikaelyan, and V.V. Sinev, Phys. Atomic Nuclei **61**, 172 (1998);  
V.I. Kopeikin, L.A. Mikaelyan, and V.V. Sinev, Phys. Atomic Nuclei **63**, 1012 (2000).

- [17] B. Kayser et al., Phys. Rev. **D 20**, 87 (1979).
- [18] G.G. Raffelt, Phys. Rev. **D 39**, 2066 (1989).
- [19] E.L. Chupp, W.T. Vestrand, and C. Reppin, Phys. Rev. Lett. **62**, 505 (1989).
- [20] V.I. Kopeikin et al., Phys. Atomic Nuclei **60**, 1859 (1997).
- [21] A.C. Dodd, E. Papageorgiu, and S. Ranfone, Phys. Lett. **B 266**, 434 (1991).
- [22] F. Bergsma et al., Phys. Lett. **B 147**, 481 (1984);  
P. Vilain et al., Phys. Lett. **B 335**, 246 (1994).
- [23] R.C. Allen et al., Phys. Rev. Lett. **55**, 2401 (1985);  
R.C. Allen et al., Phys. Rev. **D 47**, 11 (1993).
- [24] F. Reines, H.S. Gurr and H.W. Sobel, Phys. Rev. Lett. **37**, 315 (1976).
- [25] G.S. Vidyakin et al, JETP Lett. **55**, 206 (1992).
- [26] A.I. Derbin et al., JETP Lett. **57**, 769 (1993).
- [27] A.V. Kyuldjiev, Nucl. Phys. **B 243**, 387 (1984).
- [28] C. Amsler et al., Nucl. Instrum. Methods **A 396**, 115 (1997);  
C. Brogini, Nucl. Phys. **B (Procs. Suppl.) 91**, 105 (2001).
- [29] H.T. Wong and J. Li, Mod. Phys. Lett. **A 15**, 2011 (2000);  
H.B. Li et al., Nucl. Instrum. Methods **A 459**, 93 (2001).
- [30] A.G. Beda, E.V. Demidova, and A.S. Starostin, Nucl. Phys. **A 663**, 819 (2000);  
A.S. Starostin and A.G. Beda, Phys. Atom. Nucl. **63** 1297 (2000).
- [31] W. Hampel et al., Phys. Lett. **B 420**, 114 (1998);  
J.N. Abdurashitov et al., Phys. Rev. **C 59** 2246 (1999).
- [32] I.R. Barabanov et al., Astropart. Phys. **5**, 159 (1996);  
A.V. Golubchikov et al., Phys. Atom. Nucl. **59**, 1916 (1996);  
V.N. Trofimov, B.S. Neganov, and A.A. Yukhimchuk, Phys. Atom. Nucl. **61**, 1271 (1998);  
A. Ianni and D. Montanino, Astropart. Phys. **10**, 331 (1999).
- [33] V.N. Trofimov, B.S. Neganov, and A.A. Yukhimchuk, Phys. Atom. Nucl. **61**, 1271 (1998).

- [34] Letter of Intent, LENS Collaboration (1999).
- [35] F. Vannucci, in *Proc. of Neutrino Telescope Workshop, 1999*, ed. M. Baldo-Ceolin, Vol. **1**, 165 (1999).
- [36] T.L. Jenkins, F.E. Kinard, and F. Reines, *Phys. Rev. Lett.* **185**, 1599 (1969);  
E. Pasierb et al., *Phys. Rev. Lett.* **43**, 96 (1979);  
G.S. Vidyakin et al., *JETP Lett.* **49**, 151 (1988);  
G.S. Vidyakin et al., *JETP Lett.* **51**, 279 (1990);  
S.P. Riley et al., *Phys. Rev.* **C 59**, 1780 (1999).
- [37] H.C. Lee, *Nucl. Phys.* **A 294**, 473 (1978) ;  
T.W. Donnelly and R.D. Peccei, *Phys. Rep.* **50**, 1 (1979).
- [38] L.M. Krauss, S.L. Glashow, and D.N. Schramm, *Nature* **310**, 191 (1984).
- [39] B. Armbruster et al., *Phys. Lett.* **B 423**, 15 (1998).
- [40] J. Bernabéu et al., *Nucl. Phys.* **B 378**, 131 (1992);  
K. Kubodera and S. Nozawa, *Int. J. Mod. Phys.* **E 3**, 101 (1994).
- [41] H.T. Wong et al., *Astropart. Phys.* **14**, 141 (2000).

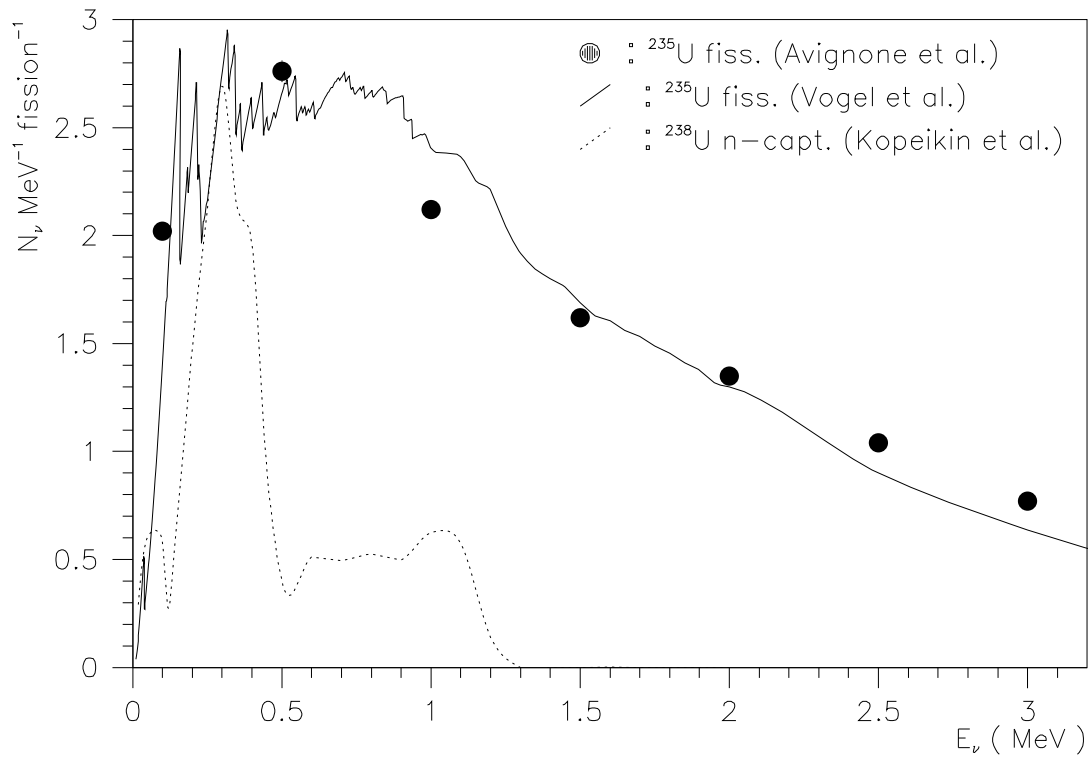
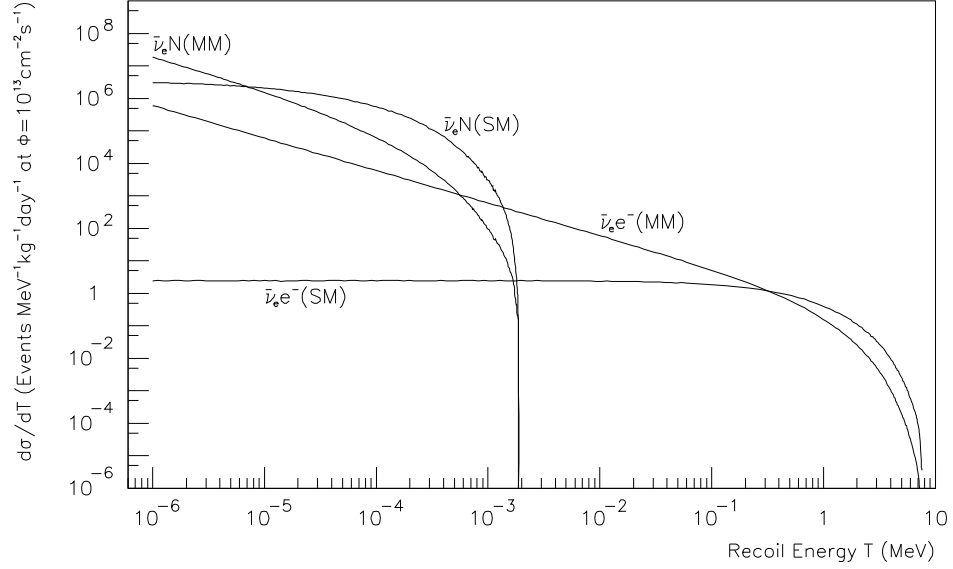


Figure 1: Calculated low energy reactor neutrino spectra due to fission from Refs. [6] and [12], and that due to  $\beta$ -decays following neutron capture on  $^{238}\text{U}$  from Ref. [11].

(a)



(b)

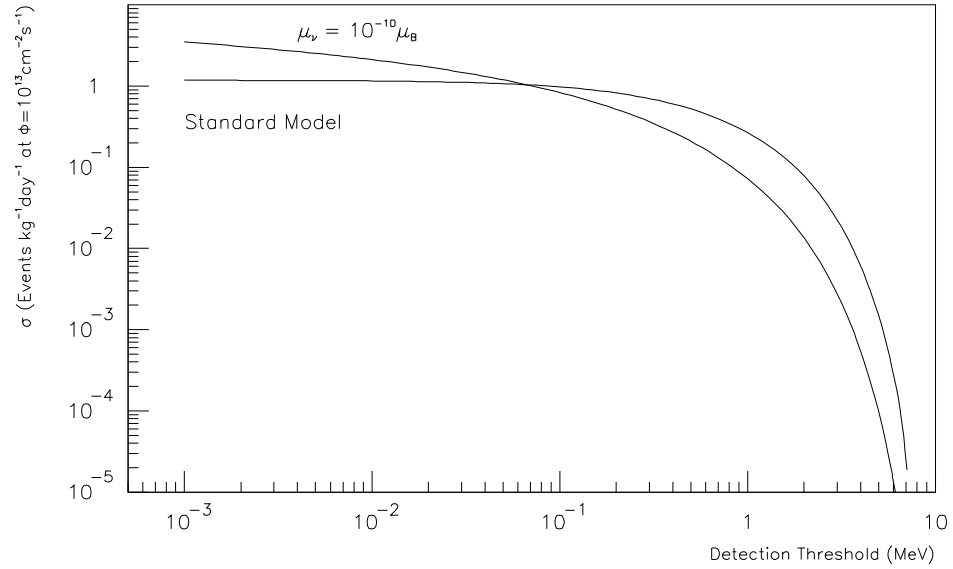
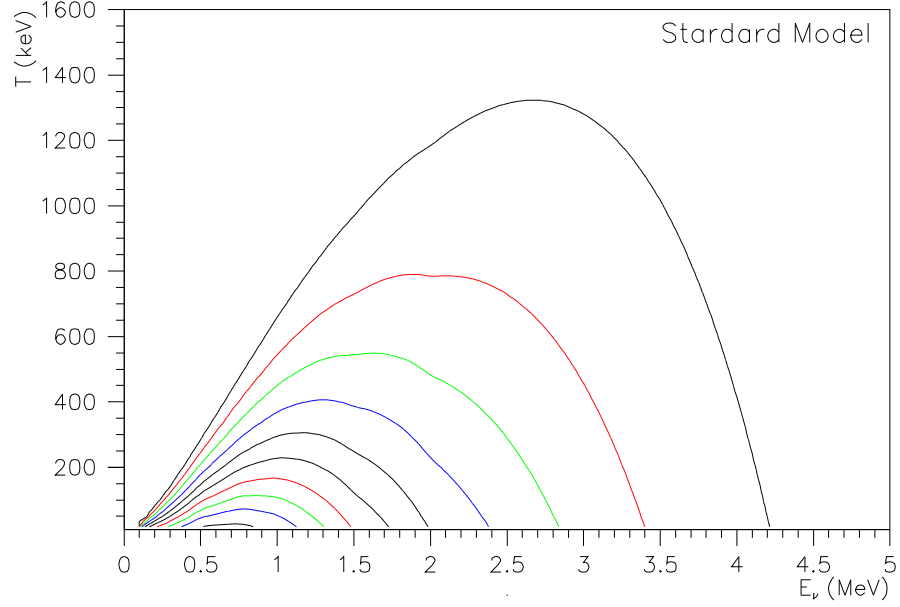


Figure 2: (a) Differential cross section showing the recoil energy spectrum in  $\bar{\nu}_e$ -e and coherent  $\bar{\nu}_e$ -N scatterings, at a reactor neutrino flux of  $10^{13} \text{cm}^{-2} \text{s}^{-1}$ , for the Standard Model processes and due to a neutrino magnetic moment of  $10^{-10} \mu_B$ . (b) The integral event rates as a function of the detection threshold of the recoil electrons in the  $\bar{\nu}_e$ -e processes.

(a)



(b)

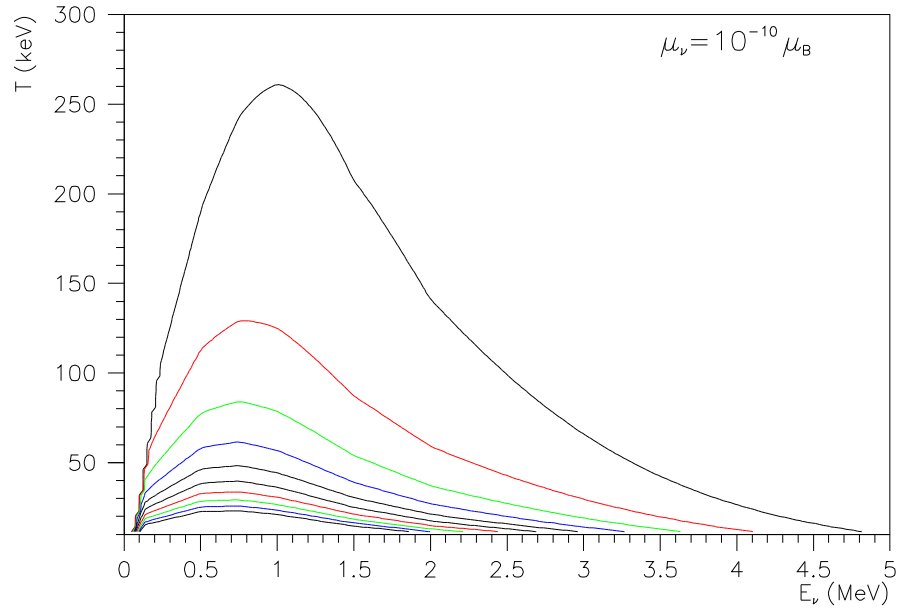
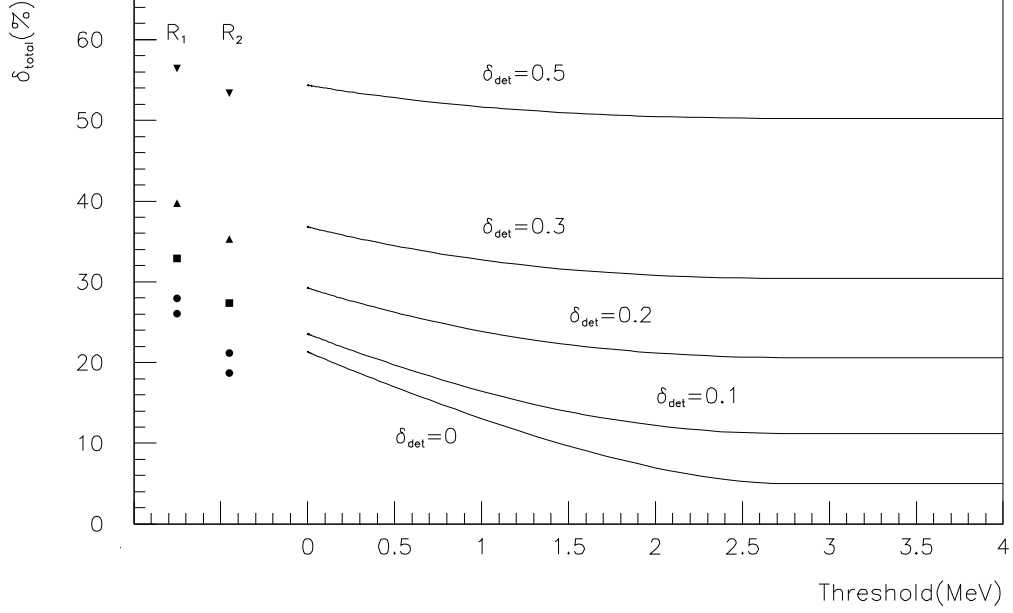


Figure 3: Correlation plots for recoil energy ( $T$ ) versus neutrino energy ( $E_\nu$ ) for (a) Standard Model and (b) Magnetic Moment contributions due to  $\bar{\nu}_e$ -e scattering from the reactor. Adjacent contours represent equipartition levels of event rates normalized to the innermost contour. Magnetic scatterings are due mostly to low energy neutrinos giving rise to low energy electron recoils.

(a)



(b)

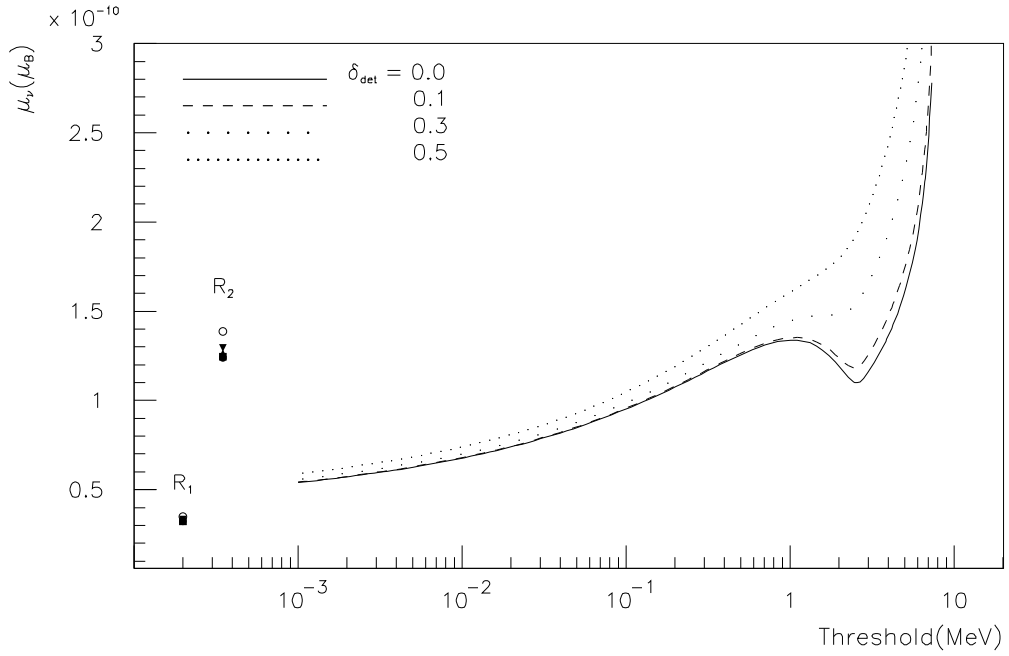
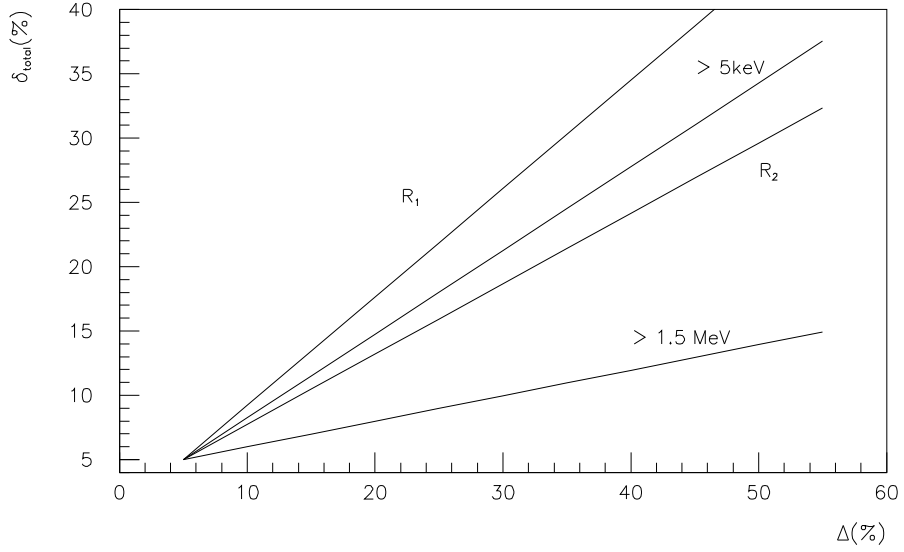


Figure 4: Attainable sensitivities in  $\bar{\nu}_e$ -e scattering experiments as a function of detection threshold for (a) SM cross section measurements and (b) MM limits at 90% CL, in the case where  $\xi=3$  MeV and  $\Delta=30\%$ , for different values of the experimental uncertainties  $\delta_{\text{det}}$ . The different symbols for the ranges  $R_1$  and  $R_2$  correspond to the different  $\delta_{\text{det}}$  values.

(a)



(b)

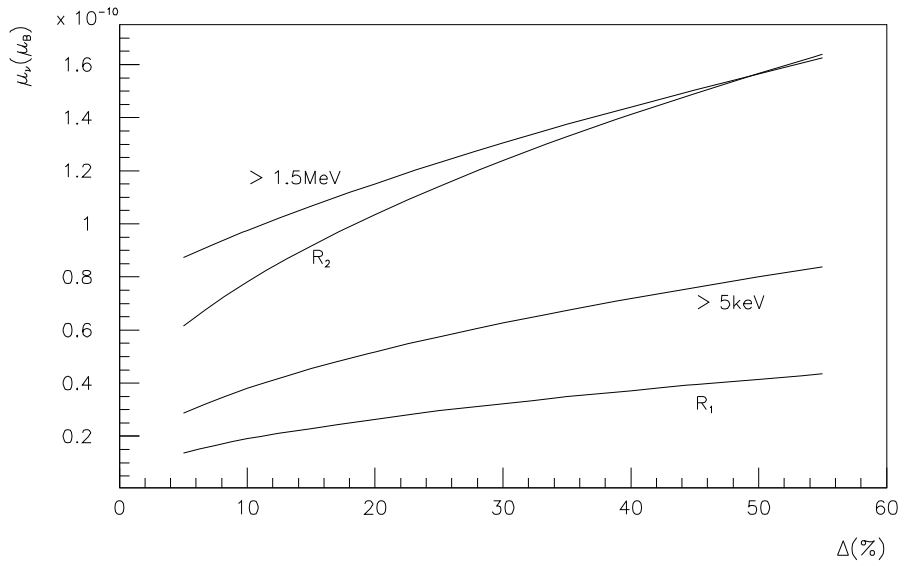


Figure 5: Attainable sensitivities in  $\bar{\nu}_e$ -e scattering experiments for (a) SM cross section measurements and (b) MM limits at 90% CL, in the case where  $\xi=3\text{ MeV}$  and  $\delta_{\text{det}}=0\%$ , as a function of  $\Delta$ , the uncertainty parameter for the low energy reactor neutrino spectra. Different contours correspond to different detection ranges.

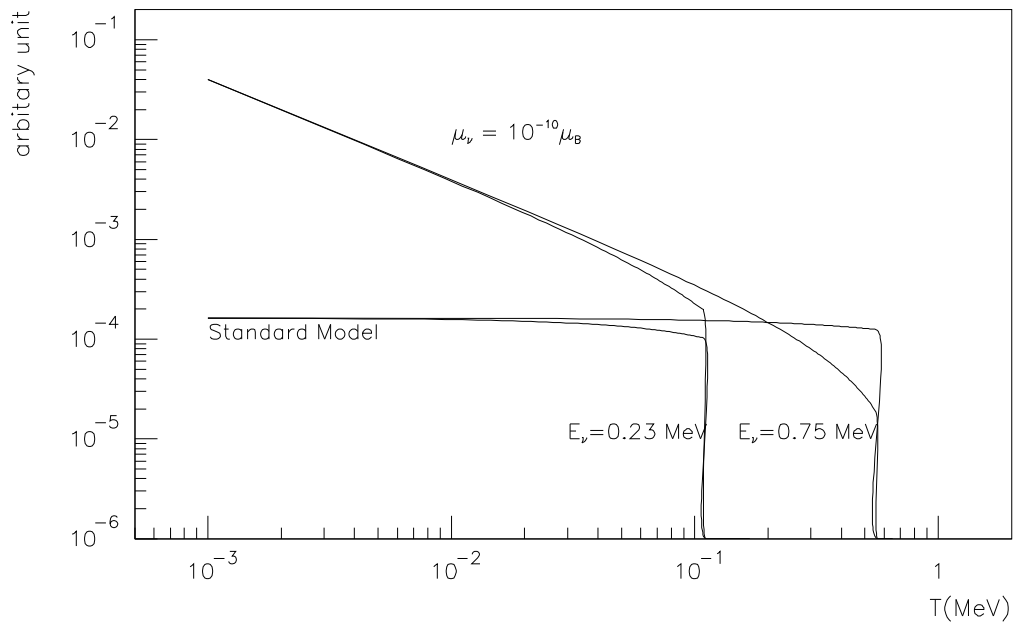


Figure 6: Differential cross sections for electron recoils in  $\nu_e$ -e scatterings due to SM and MM processes with  $^{51}\text{Cr}$  and  $^{55}\text{Fe}$   $\nu_e$  sources.

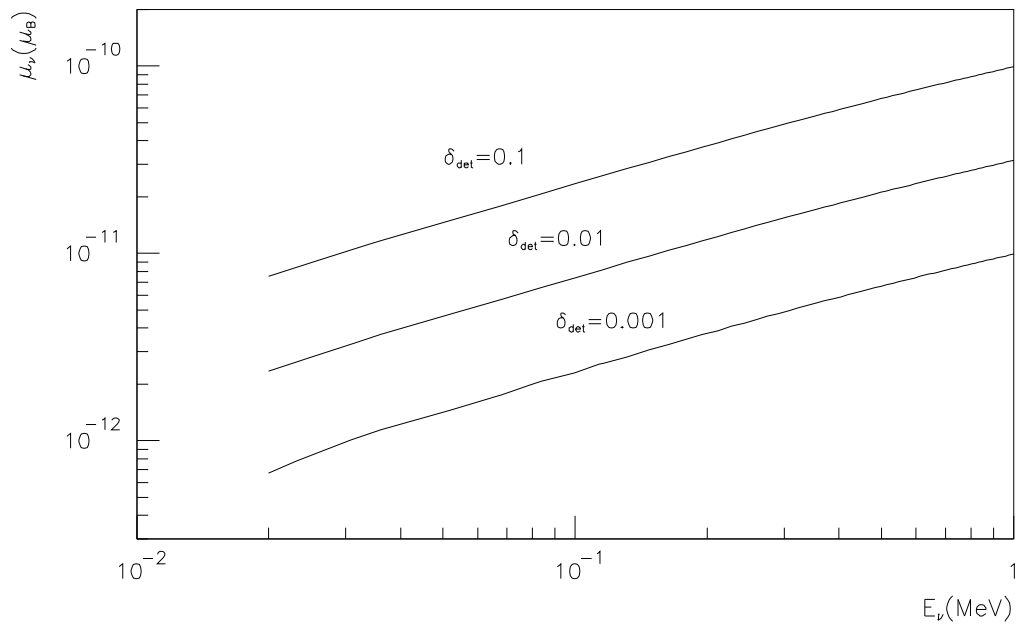


Figure 7: The attainable magnetic moment sensitivities in  $\nu_e$ -e scattering experiments as a function of  $\nu_e$  source energy at different experimental uncertainties  $\delta_{\text{det}}$ .

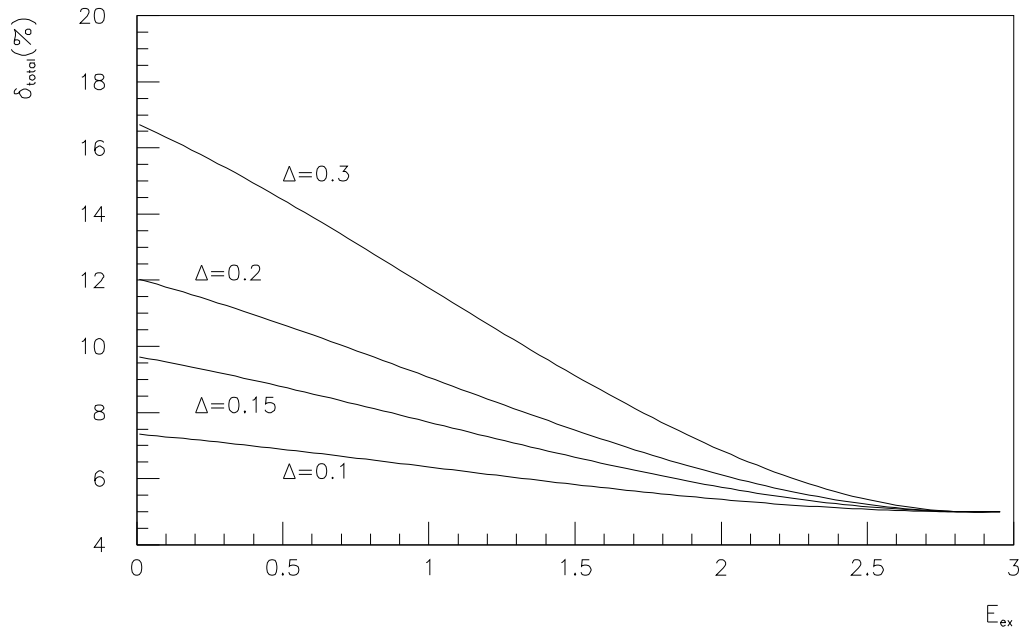


Figure 8: Attainable accuracies for reactor-based neutrino neutral-current excitation experiments as a function of the nuclear excitation threshold for different values of  $\Delta$  in the cases of *perfect* experiments ( $\delta_{\text{det}}=0\%$ ).

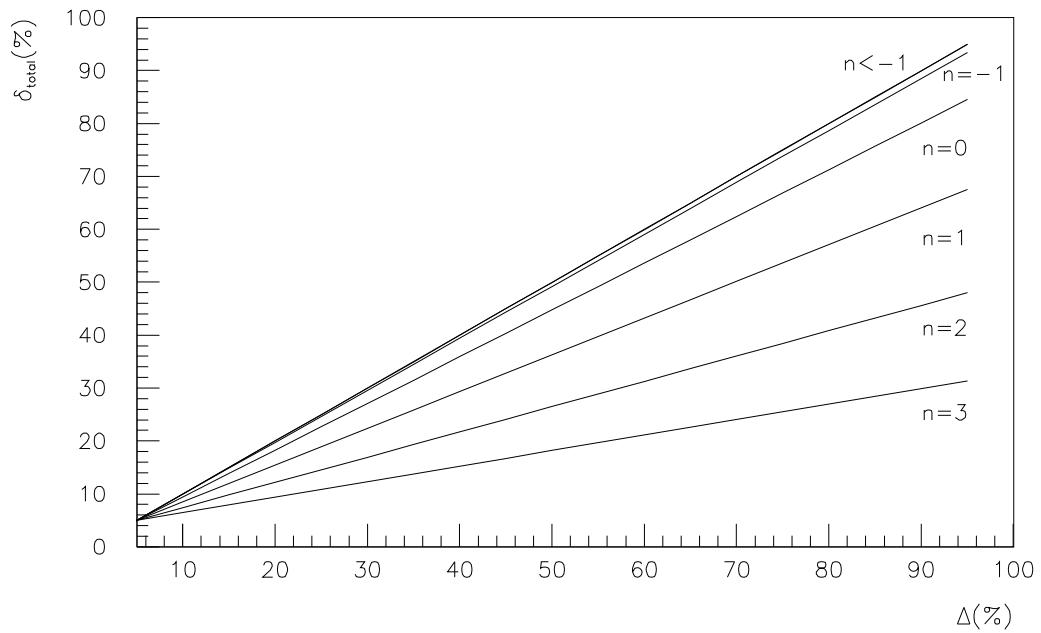


Figure 9: Attainable accuracies for cross-section measurements of reactor neutrino with nuclei where the energy dependence is parametrized by Eq. 13, as a function of index  $n$  and for various values of  $\Delta$  in the cases of *perfect* experiments ( $\delta_{\text{det}}=0\%$ ).